Available online at www.sciencedirect.com
ScienceDirect
Journal of Power Sources 175 (2008) 390–396
JOURNAL OF POWER SOURCES
www.elsevier.com/locate/jpowsour

Study on the mesocarbon microbeads/polyphenylene sulfide composite bipolar plates applied for proton exchange membrane fuel cells

Tao Yang [a,*], Pengfei Shi [b]

[a] *Department of Chemistry Engineering, Huaihai Institute of Technology, Lianyungang, 222005, China*
[b] *Department of Applied Chemistry, Harbin Institute of Technology, Harbin, 150001, China*

Received 8 July 2007; received in revised form 23 August 2007; accepted 30 August 2007
Available online 14 September 2007

Abstract

Thermoplastic/graphite composite bipolar plates based on polyphenylene sulfide (PPS) and mesocarbon microbeads (MCMB) were prepared by compression molding at a pressure of 40 MPa and 400 °C. Electrical conductivity, bulk density, flexural strength, water and ethanol absorption were determined as function of PPS content. The influences of molding time, actived carbon and carbon fiber on the properties of the composite bipolar plates were investigated, the cross section of the composite plates were analyzed by scanning electron microscope (SEM). We found that the optimized PPS content is 20 wt% and the required molding time is 30 min. In particular, the composite plates containing 20 wt% PPS demonstrated in-plane conductivity as high as 133.7 S cm^{-1}, through-plane conductivity 21.37 S cm^{-1}, in addition to showing the value of density, flexural strength, water and ethanol absorption as 1.98 g cm^{-3}, 38.82 MPa, 0.0409 and 0.352 g cm^{-3}. The addition of actived carbon degraded all the performance of the bipolar plate, while addition of carbon fiber improved almost all the performance of bipolar plate except bulk density and through-plane conductivity. The performances of fuel cell with this composite bipolar plate were tested, no distinct variation occurred after the composite plates operating in fuel cell. These data indicates the chemical and mechanical stability of the composite plates and their potential application in fuel cell.

Keywords: Proton exchange membrane fuel cell; Polyphenylene sulfide; Mesocarbon microbeads; Composite bipolar plate

1. Introduction

Bipolar plates are the important key components in fuel cells on the basis of their manifold function. They distribute the fuel and oxidant within the cell, separate the individual cells in the stack, conduct current away from each cell, and carry water away from each cell. Traditionally, the most commonly used bipolar material is machined graphite because it provides excellent corrosion resistance, low bulk density and high electrical conductivity [1,2], which are especially important in stationary and high power application. However, the brittleness of graphite and difficulties in machining make it hard to reduce the thickness and maintain the strength simultaneously [3]. On the other hand, the cost of machining flow channels cannot be reduced effectively up to now. Numerous materials as alternatives to graphite plates have been developed and studied to reduce the cost as well as the weight of the fuel cell.

Metals such as stainless steel and metal alloys are good substitutes for graphite, which offer lower electrical resistance, higher mechanical strength, zero gas permeability and much superior productivity [4,5]. Nevertheless, metal plates are prone to corrosion or dissolution by exposing to an operating environment with a pH 2–3 at temperature around 80 °C. Firstly, dissolved metal ion may result in the proton exchange membrane poisoning and hence lowering the proton conductivity. On the other hand, a corrosion layer on the metal surface may increase the interface contact resistance. A protective layer is needed to solve this problem [6–8]. Wang et al. [9] modified the native passive oxide film on AISI446 by thermal nitridation at 1100 °C for 2 h, obtained high corrosion resistance and low interfacial

* Corresponding author.
E-mail address: yangtao_hit@163.com (T. Yang).

0378-7753/$ – see front matter © 2007 Elsevier B.V. All rights reserved.
doi:10.1016/j.jpowsour.2007.08.113

contact resistance. They confirmed that a protective and conductive layer may be not necessarily pinhole-free. But it is not clear whether this method can be induced in other metal plates.

Carbon/polymer composite materials with lower cost and higher flexural strength can be fabricated into any shape and size, which makes them more attractive for PEMFC stacks [10,11]. Middelman et al. [12] have investigated the attributes of the conductive composite bipolar plates and analyzed the feasibility of faster and large-scale production detailed. Much attention has been concentrated on the preparation of carbon/polymer composite. For example, Researchers in Los Alamos National Laboratory (LANL) prepared the composite bipolar plates based on graphite powder and thermosetting resin by compress molding, the conductivity was 85 S cm^{-1}, tension strength and flexural strength were 25 and 38 MPa, respectively [13]. The composite plates developed by Cho et al. [14] offered long term performances comparable to the graphite plates. Emanuelson et al. [15] obtained the 0.75 mm composite plates containing 50 wt% phenol resins, which have been operating on the 40 kW station 2 years. Wolf and Willert-Porada [16] manufactured composite plates containing 40 wt% carbon powder, they presented light weight and high conductivity.

Great effort has also been devoted to the molding technique of composite plates. Injection molding the composite plates based on thermoplastic and carbon component was reported by Heinzel et al. [17]. Kuan et al. [10] developed vinyl ester-graphite composite bipolar plates by a bulk-molding compound process, which offered the similar properties to graphite plates.

Both thermoplastic [18] and thermosetting resins [19] have been considered for development of carbon-based composite plates. Maheshwari et al. [20] manufactured the composite plates with 65 vol.% nature graphite, 25 vol.% PE and 10 vol.% other mixture (carbon fiber and carbon black), the flexural strength and mold were 81 MPa and 20 GPa, respectively. Balko and Lawrance [21] obtained the composite plates based on PVDF, graphite powder and carbon fiber, the electrical conductivity was 109 S cm^{-1}, satisfied the requirement of fuel cell.

Much work has been devoted to investigate the factors which influence the performance of composite plates such as the binder resin types [22], the size, distribution and array of conductive particles [23,24], the mixture of raw material [25], the crystallization of composite [26] and microstructure [27]. The recent paper [28] reported that the composite plates containing expendable graphite and vinyl ester had excellent electrical conductivity; however, the phase separation occurred in the plates.

PPS is an excellent thermoplastic with good mechanical properties and high corrosion resistance at high temperature. Huang et al. [29] prepared the formable sheets containing PPS by a wet-lay (paper making) process, subsequently stacked and compressed mold to form bipolar plates. It is claimed that the PPS-based bipolar plate was the first polymer composite bipolar plate to meet industrial requirements for tensile and flexural properties. Cunnigham et al. [30,31] improved the through-plane conductivity of the PPS-based plates by laminating a polyvinylidene fluoride/graphite skin layer or a PPS/graphite skin layer on the PPS-based wet-lay material core. This manufacture process takes a little longer time and relatively complex. In this study, MCMB/PPS composite plates was prepared by compression molding at 400 °C to confirm the usability of simple manufacture process and to find the new substitute for graphite plates. The influences of PPS content, molding time, actived carbon and carbon fiber on the properties of the composite bipolar plates were investigated in detail.

2. Experimental

2.1. Pretreatment of raw material

PPS (<100 μm, Chengtu letian Plastic Co., Ltd., China), MCMB(<100 μm, Harbin Coslight Power Co., Ltd., China), actived carbon (<180 μm, Harbin Coslight Power Co., Ltd., China), carbon fiber (<120 μm, Harbin Coslight Power Co., Ltd., China) were dried in oven, weighed and mixed according to the scheduled prescription (Table 1). The mixture was firstly triturated to gray-black powder in the carnelian mortar, then grinded many times to jet-black powder, which was subsequently sieved to 100 and 200 meshes. The mixture powder was finally dried at 120 °C in oven for 5 h.

2.2. Preparation of carbon/polymer composite bipolar plate

The molds were pre-heated to 120 °C beforehand. The dried mixtures were weighed and displayed in the molds. The pressure was increased to 40 MPa at the rate of 0.1 MPa s^{-1}, the mold and composite was heated to 400 °C from room temperature at the rate of 1 °C s^{-1} subsequently. The temperature was maintained at 400 °C for 30 min by compensating heat, the mold and the molded bipolar plates were then cooled to room temperature. The surface of the molded bipolar plate was polished before the following tests.

2.3. Characterization of composite plates

All composites plates were characterized by bulk density, electrical conductivity, flexural strength, absorption to water and ethanol.

The electrical conductivity of the composite plate was measured by the four-probe technique. The electrical conductivity was calculated from the value of electrical resistance. An average of 5–7 records on each plate was reported in this paper. The

Table 1
The scheduled prescription of composite plates

Samples	MCMB (wt%)	PPS (wt%)	Actived carbon (wt%)	Carbon fiber (wt%)
1	85	15	–	–
2	83	17	–	–
3	80	20	–	–
4	77	23	–	–
5	75	25	–	–
6	70	30	–	–
7	75	20	5	–
8	75	20	–	5

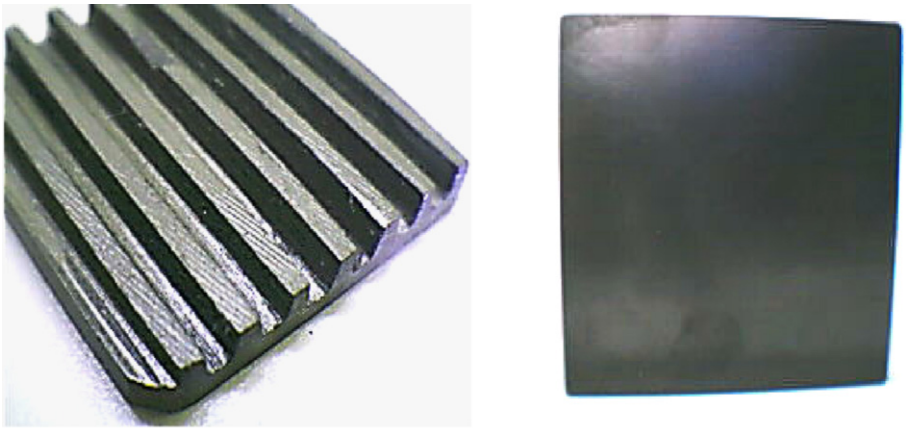

(a) Composite plate with flow channels (b) Composite plate without flow channels

Fig. 1. The bipolar plates made in our laboratory. (a) Composite plate with flow channels; (b) composite plate without flow channels.

flexural strength was measured by three point bending technique, the dimension of samples in flexural strength test was 100 mm × 10 mm × 2 mm.

The performance of the cells with the composite plates and with the graphite plates were compared to investigate the effect of practical cell operating on the composite plates, the mechanical properties and electrical properties of the composite plates were characterized before and after operating in the fuel cell.

3. Results and discussion

3.1. Molding process of composite plate

The contact of MCMB and PPS power became tight with the increase of pressure. PPS melted when the temperature increased to the melting point and the solid–liquid mixture thus came into being. Aperture decreased due to the compression, some holes disappeared, and the composite plates formed when the mold cooled. The as formed composite plates are shown in Fig. 1.

3.2. Physical and mechanical properties of composite plates

Considering the ease of molding, the PPS content varied from 15 to 30 wt% based on the pre-experimental (not mentioned here). The bulk density and in-plane conductivity were largely influenced by the PPS content and the microstructure of the composite plates. In Fig. 2, the PPS content was increased from 15 to 30 wt%. It is seen that the electrical conductivity decreased with the increase of PPS content. The conductivity decreased monotonically from 153.5 S cm^{-1} down to 133.7 S cm^{-1} with the increase of PPS content from 15 wt% up to 20 wt%, and then dropped sharply to 81.7 S cm^{-1} at 23 wt% PPS. The decrease of conductivity can be attributed to the increase of the local concentration of insulated resin matrix among MCMB particles, restricts the electron conducting pathways.

One may argue that PPS content 15 wt% should be used to capitalize on very high electrical conductivity. However, the bulk density and flexural strength (discussed in the following) were found to be poor when the PPS content was below 20 wt%. The results in Fig. 2 show that the bulk density decreased from 1.98 g cm^{-3} down to 1.798 g cm^{-3} with increasing PPS content from 20 wt% up to 30 wt%. However, the bulk density increased with the increase of PPS content from 15 wt% up to 20 wt%. The bulk density of polymer composites is assumed to depend on two contributions: (1) the content of MCMB with high bulk density; (2) the extent to which the space among the MCMB particles is filled by PPS. The max bulk density appeared at 20 wt% PPS due to the balance of above factors.

Fuel cells such as PEMFC will produce water while it is operating. Fig. 3 shows that the absorption of composite plates to water and ethanol decreased with the increase of PPS content. The more hydrophobic PPS used, the more MCMB particles surface were coated, which increased the hydrophobic ability of the composite plates. However, the absorption to water was invariable when PPS content was above 20 wt%, the absorption to ethanol dropped tardily when PPS content was above 25 wt%. Maybe, the absorption limit reached when the PPS content is above the turn point; the superfluous PPS has no contribution to the proof ability of the composite plates.

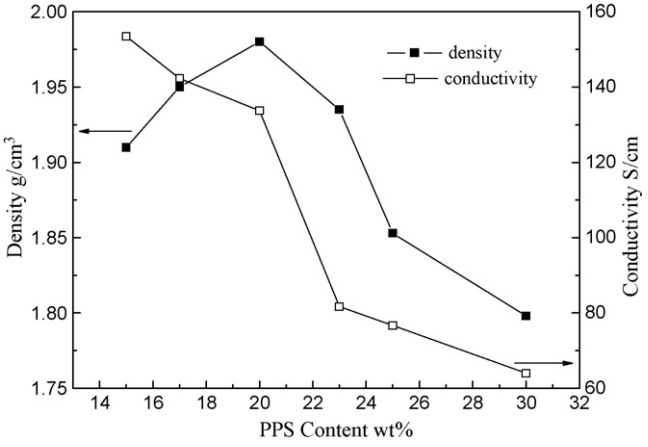

Fig. 2. Effect of PPS content on density and in-plane conductivity.

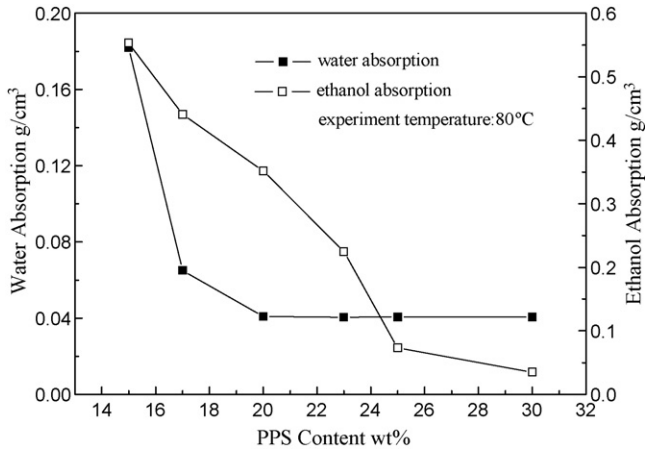

Fig. 3. Effect of PPS content on water and ethanol absorption.

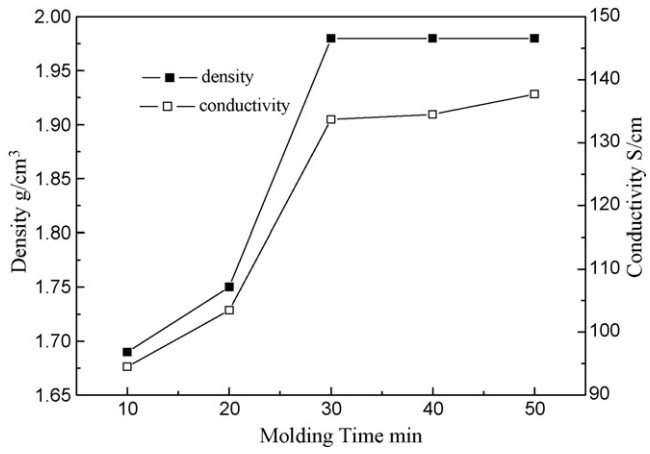

Fig. 5. Effect of molding time on density and in-plane conductivity.

Fig. 4 shows the influence of PPS content on the flexural strength of composite plates. It is seen that the flexural strength increased sharply from 23.04 MPa up to 38.82 MPa with the increase of PPS content from 15 wt% up to 20 wt%. These results indicate that the major influence on the flexural strength is PPS content. It is noteworthy that the PPS content exceeded 20 wt%, the increment of flexural strength was only 5.87 MPa at 30 wt% PPS. We observed the turn point at 20 wt% PPS by considering the influence of PPS content on flexural strength (Fig. 4) and bulk density (Fig. 2) synthetically. It is postulated that the PPS is insufficient (below 20 wt%) to fill the space among MCMB particles fully, the flexural strength and bulk density sharply increased with the increase of PPS content. While the superfluous PPS (above 20 wt%) decrease the bulk density and has no obvious contribution to the flexural strength.

3.3. Influence of molding time

Molding time referred to the period the highest temperature and pressure was held. In this experiment, all samples containing 20 wt% PPS and 80 wt% MCMB, were manufactured by the same process except the molding time.

Table 2
Effect of molding time on water and ethanol absorption

Molding time (min)	Water absorption ($g\,cm^{-3}$)	Ethanol absorption ($g\,cm^{-3}$)
10	0.0423	0.374
20	0.0415	0.368
30	0.0409	0.352
40	0.0389	0.337
50	0.0388	0.335

The dependence of density and in-plane conductivity on molding time is shown in Fig. 5. It is seen that the bulk density and electrical conductivity increased with the increase of molding time from 10 min up to 30 min. While no obvious variation on bulk density and electrical conductivity occurred when the molding time exceed 30 min. These results indicate that 30 min is sufficient to establish compact structure and electron conducting pathways in the composite plates. Table 2 shows the variation of the absorption to water and ethanol with the increase of molding time. It is seen that the influence of molding time on the absorption capability was slight. The dependence of flexural strength on molding time is shown in Fig. 6. The flexural strength sharply

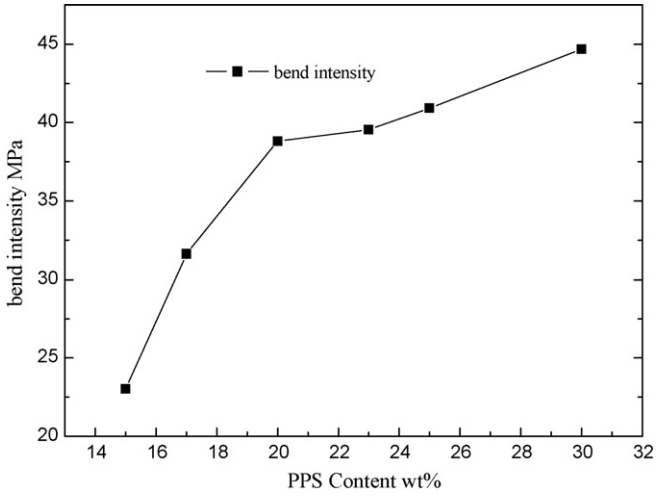

Fig. 4. Effect of PPS content on bipolar bend intensity.

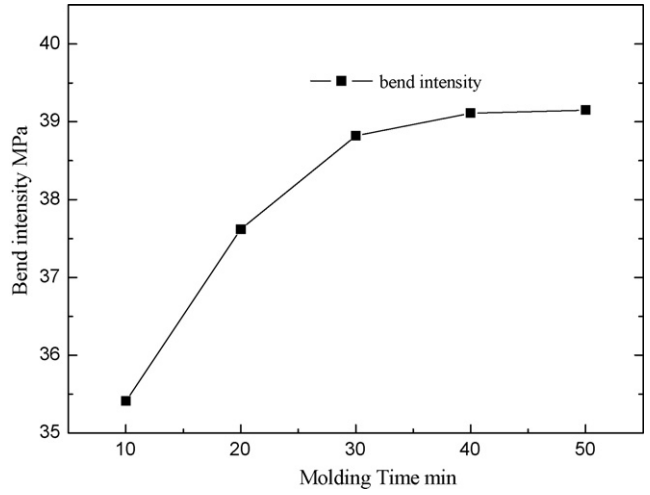

Fig. 6. Effect of molding time on bend intensity.

Table 3
Influence of actived carbon, carbon fiber addition on the composite plate

Samples	In-plane conductivity ($S\,cm^{-1}$)	Water absorption ($g\,cm^{-3}$)	Ethanol absorption ($g\,cm^{-3}$)	Bend strength (MPa)	Bulk density ($g\,cm^{-3}$)
3	133.7	0.0409	0.352	38.82	1.98
7 (adding actived carbon)	119.6	0.0522	0.567	23.09	1.76
8 (adding carbon fiber)	135.1	0.0357	0.335	41.33	1.85

3, 7 and 8 contain the same content of PPS, refer to Table 1.

Table 4
Through-plate conductivity of samples 1–8

Samples	1	2	3	4	5	6	7	8
Conductivity ($S\,cm^{-1}$)	22.79	22.52	21.37	15.77	13.63	9.31	19.75	20.91

increased from 35.41 MPa up to 38.82 MPa with the increase of molding time from 15 to 30 min. However, it is noteworthy that the flexural strength increased only 0.93 MPa when the molding time increased from 30 to 50 min. These results show that 30 min was enough to obtain the firm crosslink structure in composite plates.

3.4. Influence of actived carbon and carbon fiber addition

Table 3 shows the influence of actived carbon and carbon fiber. It can be concluded that carbon fiber can improve almost all the performance of composite plates except bulk density and through-plane conductivity, while actived carbon can degrade the composite plates.

Table 4 shows the through-plate conductivity of the samples 1–8. The results show that the through-plate conductivity decreased from 22.79 S cm^{-1} down to 9.31 S cm^{-1} with increasing the PPS content (from 1 to 6) from 15 to 30 wt%. The decrease of through-plate conductivity can be attributed to the increase of the local concentration of insulated resin matrix among the MCMB particles, restricts the electron conducting pathways. Compared to the sample 3, samples of 7 and 8 provided lower conductivity with actived carbon or carbon fiber. It is postulated that the addition of actived carbon and carbon fiber offer poor electron contact with MCMB particles.

3.5. Microstructure of composite plate

Fig. 7 shows the scanning electron micrographs of composite plate magnified 180 times and 1000 times. The samples in this experiment contained 80 wt% MCMB and 20 wt% PPS. The micrograph in Fig. 7a revealed the compact contact of MCMB particles and the even distribution of PPS around MCMB particles. The scraggy surface can be observed, which was formed during the preparation of optical micrograph sample (despite of polishing process). Fig. 7b shows the micrograph of composite plates magnified 1000 times, the dimensions of MCMB was about 20 μm. The PPS conglutination region (white region) around MCMB particles can be observed, which formed during the hot-press process, had much contribution to physical and mechanical properties of composite plates.

More MCMB particles were coated and separated with the increase of PPS content, hence the electron movement among MCMB particles was restricted. However, the more PPS improved the adhesion among the MCMB particles and increased the flexural strength effectively. Numerous interspaces formed when deflected spherical MCMB particles were piled up. The flexural strength and bulk density sharply increased with the increase of PPS content when the PPS (below 20 wt%) was insufficient to fill the interspaces fully. While the superfluous PPS (above 20 wt%) decreased the bulk density and had no obvious contribute to the flexural strength.

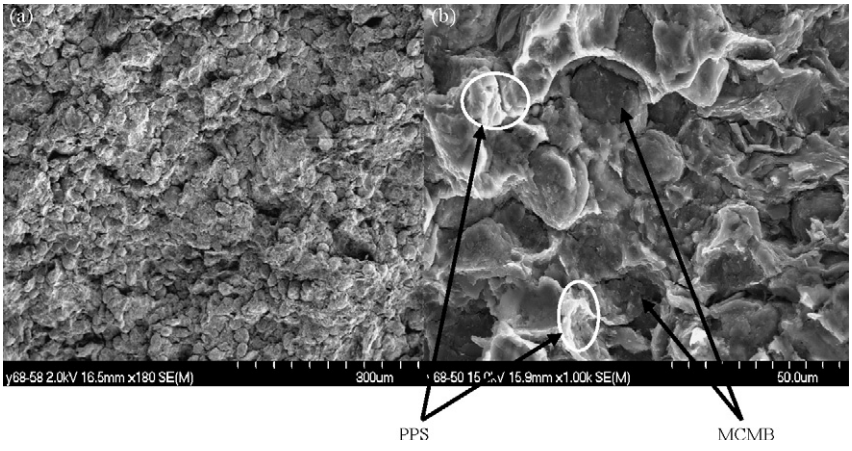

Fig. 7. Cross section micrograph of composite plates.

Table 5
Physical and mechanical properties variation of composite plates

Component	Conductivity (S cm^{-1})	Water absorption (g cm^3)	Ethanol absorption (g cm^{-3})	Bend strength (MPa)	Bulk density (g cm^{-3})
Before operating in cell	133.7	0.0409	0.352	38.82[a]	1.98
After operating in cell	132.6	0.0411	0.347	38.17	1.98

[a] The value of bend strength is referred to Table 2.

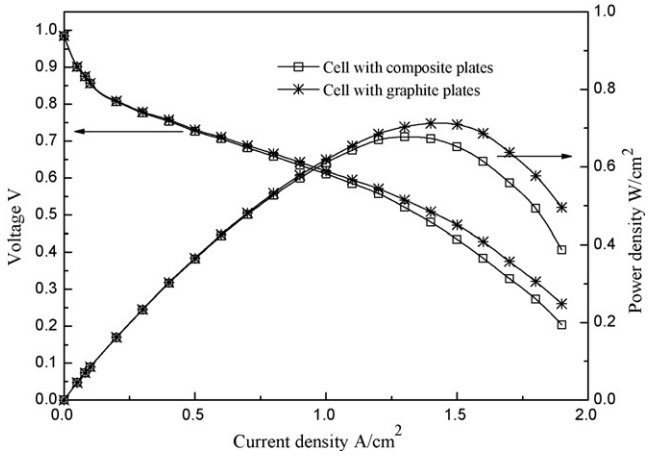

Fig. 8. *I–V* curves of cells with composite and graphite plates.

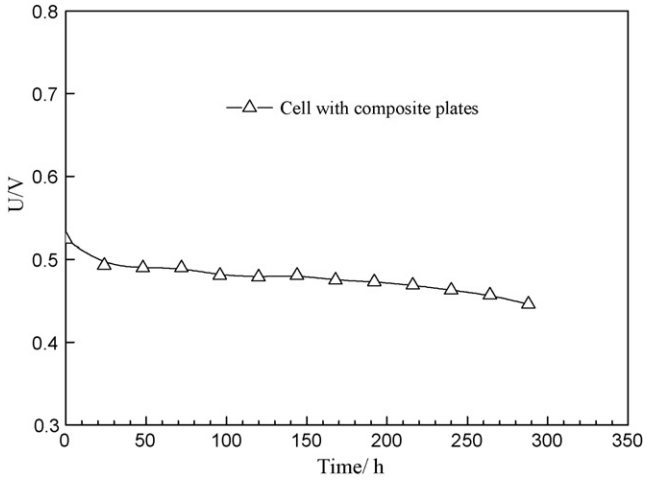

Fig. 10. *t–V* curves of cells with composite plates under 1.3 A cm^{-2}.

3.6. Cell operation characteristics of composite plate

Figs. 8–10 shows the performance of the fuel cell with the composite plates containing 80 wt% MCMB and 20 wt% PPS.

Polarization curves in Fig. 8 shows the comparison of the cells with composite plates and graphite plates. Same material and method were used to prepare the membrane electrode assembles to display the difference between the composite plate and the graphite plates. Hydrogen and oxygen were heated to 65 °C and supplied at stoichiometric 1.5, the temperature of cells was controlled at 60 °C.

From *I–V* characteristics it is observed that the power density of the cell with composite plates continuously increased up to the current density 1.3 A cm^{-2} corresponding to the maximum power density of. 677 mW cm^{-2}. The maximal power density of the cell with graphite was 713 mW cm^{-2} at the current density of 1.4 A cm^{-2}. Below 1.1 A cm^{-2} the polarization curves of the cell with composite plates was similar to that of the cell with graphite plates. However, the cell with graphite plates provided higher voltage than the cell with composite plates as the current density increased from 1.1 A cm^{-2} up to 1.9 A cm^{-2}. It is more likely results from that the insulated PPS is located on the composite plates surface, hence increases the interface contact resistance and drops the cell voltage.

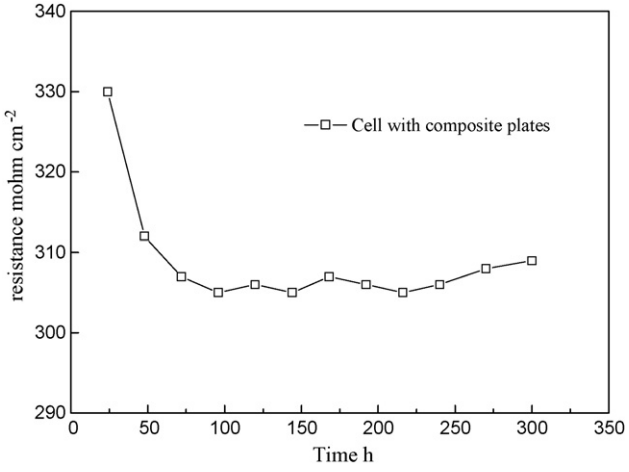

Fig. 9. Resistance of cells with composite plates.

Fig. 9 shows the cells resistances at different operation time. The cell with composite plates had larger initial resistance when the test started, and the resistance decreased continuously to 305 mΩ when the cell operated 100 h. The resistance variation may be due to the hydration of MEA by the product water. In the following time, the resistance was invariable.

Fig. 10 shows the *t–V* characteristics of cell with composite plates. Except the initial voltage point of 0.524 V, the voltage dropped from 0.493 to 0.446 V in 288 h, only 0.047 V declined.

After operating 288 h in fuel cell, the composite plates were taken apart, washed in distill water and dried in oven. Physical and mechanical properties of the composite plates were tested and shown in Table 5. It is indicated that no obvious change occurred after the composite plate experience the cell operation 288 h.

4. Conclusion

Composite plates containing MCMB and PPS powder were prepared by compression molding technique at a pressure of 40 MPa and 400 °C. The data on electrical and mechanical

properties indicate that the suitable PPS content was 20 wt%. Polarization and *t*–*V* characteristic shows the potential application of MCMB/PPS composite plates in fuel cell. No variation on electrical and mechanical properties occurred after operating in fuel cell, which indicates the stability against the acid environment at the fuel cell operating temperature (60 °C).

References

[1] G.O. Mepsed, J.M. Moore, Handbook of Fuel Cells-Fundamentals. Technology and Applications, John Wiley and Sons, Ltd., New York, 2003, pp. 286–293.
[2] A.A. Kulikovsky, J. Power Sources 160 (2006) 431–435.
[3] O.A. Velev, D.T. Tran, J.J. Kakwan, S. Gamburzev, F. Sinoneaux, S. Srinivasan, Effect of bipolar plate materials on PEMFC performance, in: 190th Fall Meeting of the Electrochemical Society, San Antonio, TX, October, 1996, p. 101 (abstract).
[4] S.-T.K. Hong, K.S. Weil, J. Power Sources 168 (2007) 408–417.
[5] J. Wind, A. LaCroix, S. Braeuninger, P. Hedrich, C. Heller, M. Schudy, Handbook of Fuel Cells-Fundamentals. Technology and Applications, John Wiley and Sons, Ltd., New York, 2003, pp. 295–307.
[6] Y. Wang, D.O. Northwood, J. Power Sources 163 (2006) 500–508.
[7] R. Tian, J. Sun, L. Wang, Int. J. Hydrogen Energy 31 (2006) 1874–1878.
[8] M.P. Brady, K. Weisbrod, C. Zawodzinski, I. Pailauskas, R.A. Buchanan, Electrochem. Solid-State Lett. 5 (2002) A245–A247.
[9] H. Wang, M.P. Brady, K.L. More, H.M. Meyer III, J.A. Turner, J. Power Sources 138 (2004) 79–85.
[10] H.-C. Kuan, C.-C.M. Ma, K.H. Chen, S.-M. Chen, J. Power Sources 134 (2004) 7–17.
[11] A. Hermann, T. Chaudhuri, P. Spagnol, Int. J. Hydrogen Energy 30 (2005) 1297–1302.
[12] E. Middelman, W. Kout, B. Vogelaar, J. Lenssen, E. de Waal, J. Power Sources 118 (2003) 44–46.
[13] D.N. Busick, S. Wilson, Mater. Res. Soc. Symp. Proc. 575 (2000) 247–251.
[14] E.A. Cho, U.-S. Jeon, H.Y. Ha, S.-A. Hong, I.-H. Oh, J. Power Sources 125 (2004) 178–182.
[15] R.C. Emanuelson, W.L. Luoma, William A. Taylor, US 4,301,222 (1981).
[16] H. Wolf, M. Willert-Porada, J. Power Sources 153 (2006) 41–46.
[17] A. Heinzel, F. Mahlendorf, O. Neimzig, C. Kreuz, J. Power Sources 131 (2004) 35–40.
[18] M.K. Bisaria, P. Adrin, M. Abdou, Y. Cai, US 6,379,795 (2002).
[19] J.-G. Wang, Q.-G. Guo, L. Liu, J.-R. Song, Carbon 40 (2002) 2447–2452.
[20] P.H. Maheshwari, R.B. Mathur, T.L. Dhami, J. Power Sources 173 (2007) 394–403.
[21] E.N. Balko, R.J. Lawrance, US 4,339,322 (1982).
[22] R. Tchoudakow, O. Breuer, M. Narkis, Polym. Eng. Sci. 36 (1996).
[23] A. Malliaris, D.T. Turner, J. Appl. Phys. 42 (1971).
[24] R.H.J. Blunk, C.L. Tucker, Y. Yoo, D.J. Lisi, US 6,607,857 (2003).
[25] E.K. Sichel, Carbon Black-Polymer Composites, Marcel Dekker, New York, 1982.
[26] M. Zhang, W. Jia, X.J. Chen, J. Appl. Polym. Sci. 62 (1996) 743.
[27] J.C. Grunlan, W.W. Gerberich, L.F. Francis, J. Appl. Polym. Sci. 80 (2001) 692–705.
[28] M. Abd Elhamid, R.H.J. Blunk, Y.M. Mikhail, D.J. Lisi, US 03,272,199 (2003).
[29] J. Huang, D.G. Baird, J.E. McGrath, J. Power Sources 150 (2005) 110–119.
[30] B.D. Cunningham, D.G. Baird, J. Power Sources 168 (2007) 418–425.
[31] Brent D. Cunningham, J. Huang, D.G. Baird, J. Power Sources 165 (2007) 764–773.